Fibers and Polymers 2016, Vol.17, No.10, 1579-1588
DOI 10.1007/s12221-016-6689-z

ISSN 1229-9197 (print version)
ISSN 1875-0052 (electronic version)

Preparation of Electroconductive, Magnetic, Antibacterial, and Ultraviolet-blocking Cotton Fabric Using Reduced Graphene Oxide Nanosheets and Magnetite Nanoparticles

Mohammad Mirjalili*

Department of Textile Engineering, Yazd Branch, Islamic Azad University, Yazd, Iran
(Received June 28, 2016; Revised August 22, 2016; Accepted August 24, 2016)

Abstract: The main goal of present study was the fabrication of cotton fabric with special functions, including electrical conductivity, magnetic, antibacterial, and ultraviolet (UV) blocking. In this regard, the cotton fabric was primarily coated with graphene oxide and then reduction of graphene oxide and synthesis of magnetite nanoparticles accomplished in one step. The alkaline hydrolysis of magnetite precursors and reduction of graphene oxide was simultaneously performed using sodium hydroxide to produce reduced graphene oxide/Fe_3O_4 nanocomposite on the fabric surface. The prepared cotton fabrics were characterized with field emission scanning electron microscope (FE-SEM), X-ray diffraction (XRD), energy dispersive X-ray spectroscopy (EDS), and X-ray photoelectron spectroscopy (XPS). The treated fabrics with reduced graphene oxide/Fe_3O_4 nanocomposite displayed a low electrical resistivity i.e. 80 kΩ/sq. Furthermore, the coated fabrics showed reasonable magnetic properties due to the presence of magnetite nanoparticles on the surface of cotton fabrics. Moreover, this process imparted proper antibacterial properties and UV blocking activity to cotton samples.

Keywords: Reduced graphene oxide, Magnetite nanoparticles, Cotton, Electrical conductivity, Magnetic, Antibacterial

Introduction

Magnetite (Fe_3O_4) nanoparticles have attracted attentions due to its strong superparamagnetic property, high adsorption ability, electronic properties, antibacterial activity, low toxicity, low cost and high bio-compatibility [1-5]. Fe_3O_4 nanoparticles have potential in important applications such as targeted drug delivery [6], cancer therapy [7], microwave absorption [8], electromagnetic interference (EMI) shielding [9], electromechanical actuators [10] and magnetic resonance imaging (MRI) [11]. Recently, some researchers investigated the finishing of textiles with magnetite nanoparticles. For instance, Zhang and Zhu produced magnetic polyamide fabrics using Fe_3O_4 nanoparticles [12]. Along the same lines, Li *et al.* obtained super-paramagnetic, conductive and EMI shielding fabrics based on magnetite coatings on polyester fabrics [13]. Zhang *et al.* prepared magnetic polyethylene terephthalate fabrics with Fe_3O_4 nanoparticles, which were prepared through the hydrothermal method [14]. Moreover, *in situ* synthesis of magnetite nanoparticles on polyester fabric for producing multi-functional fabric with magnetic, antibacterial and sono-Fenton catalytic activities was reported by Harifi and Montazer [15]. More recently, synthesis of magnetite nanoparticles on wool fabrics was investigated by Nazari and colleagues [16]. The treated wool fabrics exhibited magnetic and antifungal properties.

Graphene, one-atom-thick planar sheets of sp^2-bonded carbon atoms that are densely packed into a 2-D honeycomb crystal lattice, has become one of the most attractive materials due its unique chemical and physical properties as well as its diverse potential applications [17]. Some researchers coated textiles with graphene and proved significant electrical conductivity [18-23]. Qu *et al.* produced UV blocking cotton fabric using graphene [24]. Tian *et al.* obtained ductile cotton fabrics with extraordinary electrical and robust ultraviolet protective properties by depositing graphene doped poly(3,4-ethylenedioxythiophene):poly(styrenesulfonate) and chitosan upon fabric substrate [25]. Moreover, fabrication of textiles with multiple characteristics was reported through coating of graphene/metal oxides nanocomposites like graphene/TiO_2 [26-30] and graphene/SnO_2 [31] on the surface of the fabric. However, the coating of graphene/Fe_3O_4 nanocomposite on textiles has not been reported yet.

In this work, the coating of reduced graphene oxide/magnetite nanocomposite onto cotton fabric was presented for the first time. The electrical conductivity, magnetic property, antibacterial activity, and UV blocking property of the treated fabrics, and the synergism effect of reduced graphene oxide and magnetite nanoparticles on these properties and other characterization of the fabric were investigated and are discussed in detail.

Experimental

Materials

The bleached plain weave 100 % cotton fabric was used with the wrap/weft density of 30/28 yarn/cm and the fabric weight of 102 g/m^2. Graphite powder (particle size<20 μm) was purchased from Sigma-Aldrich. Iron (II) chloride tetrahydrate ($FeCl_2 \cdot 4H_2O$), iron (III) chloride ($FeCl_3$), sodium hydroxide (NaOH), sulfuric acid (H_2SO_4), potassium permanganate ($KMnO_4$), hydrogen peroxide (H_2O_2) and

*Corresponding author: dr.mirjalili@iauyazd.ac.ir

hydrochloric acid (HCl) were utilized from Merck.

Methods

Synthesis of Graphene Oxide

Graphene oxide was synthesized by a modified Hummers method as previously reported [26]. Briefly, 1 g graphite powder was added to 50 m*l* sulfuric acid under stirring for 12 h at ambient temperature. Afterward, $KMnO_4$ (3.5 g) was slowly put in an ice bath below 10 ºC and then stirred for 2 h at 50 ºC. Next, deionized water (70 m*l*) and H_2O_2 (5 m*l*) were added, and the solution was stirred for 30 min. Finally, the resultant product was centrifuged and washed successively with deionized water, 5 % HCl and deionized water again (three times). The obtained brown paste was mixed with water in various concentrations (0.1, 0.2, 0.3 and 0.5 % w/v), and then the dispersion was exfoliated in an ultrasonic bath (Euronda Eurosonic® 4D, 350 W, 50/60 Hz) for 60 min.

Coating Cotton Fabric with Graphene Oxide

The cotton samples were immersed in the aqueous suspension of graphene oxide with various concentrations

Table 1. Experimental conditions and tests results

Sample	Graphene oxide (w/v %)	$FeCl_3$ (mg)	$FeCl_2$ (mg)	NaOH (wt.%), pH	Electrical resistivity (Ω/square)	Electrical resistivity after washing (Ω/square)	Burning ash (o.w.f. %)	Burning ash after washing (o.w.f. %)	Saturation magnetization (emu g^{-1})
1	-	162	99.5	1, 10	805×10^6	-[a]	-[a]	-[a]	7.1
2	-	162	99.5	2, 11	800×10^6	-[a]	-[a]	-[a]	7.8
3	-	162	99.5	3, 12	800×10^6	-[a]	-[a]	-[a]	7.7
4	0.1	-	-	-	1.1×10^9	-[a]	-[a]	-[a]	-[a]
5	0.1	-	-	1, 10	360×10^6	-[a]	-[a]	-[a]	-[a]
6	0.1	-	-	2, 11	310×10^6	-[a]	-[a]	-[a]	-[a]
7	0.1	-	-	3, 12	300×10^6	-[a]	-[a]	-[a]	-[a]
8	0.1	162	99.5	1, 10	350×10^6	-[a]	-[a]	-[a]	7.0
9	0.1	162	99.5	2, 11	300×10^6	-[a]	-[a]	-[a]	7.1
10	0.1	162	99.5	3, 12	300×10^6	-[a]	-[a]	-[a]	7.1
11	0.2	-	-	-	1.5×10^9	-[a]	-[a]	-[a]	-[a]
12	0.2	-	-	1, 10	60×10^6	-[a]	-[a]	-[a]	-[a]
13	0.2	-	-	2, 11	40×10^6	-[a]	-[a]	-[a]	-[a]
14	0.2	-	-	3, 12	30×10^6	-[a]	-[a]	-[a]	-[a]
15	0.2	162	99.5	1, 10	5×10^6	-[a]	-[a]	-[a]	6.5
16	0.2	162	99.5	2, 11	5×10^6	-[a]	-[a]	-[a]	6.7
17	0.2	162	99.5	3, 12	2×10^6	-[a]	-[a]	-[a]	6.8
18	0.3	-	-	-	2×10^9	-[a]	-[a]	-[a]	-[a]
19	0.3	-	-	1, 10	300×10^3	-[a]	-[a]	-[a]	-[a]
20	0.3	-	-	2, 11	260×10^3	-[a]	-[a]	-[a]	-[a]
21	0.3	-	-	3, 12	220×10^3	-[a]	-[a]	-[a]	-[a]
22	0.3	162	99.5	1, 10	290×10^3	-[a]	-[a]	-[a]	6
23	0.3	162	99.5	2, 11	255×10^3	-[a]	-[a]	-[a]	6.2
24	0.3	162	99.5	3, 12	210×10^3	-[a]	-[a]	-[a]	6.2
25	0.5	-	-	-	2×10^9	-[a]	1.15	0.48	-[a]
26	0.5	-	-	1, 10	180×10^3	180×10^3	1.11	1.07	-[a]
27	0.5	-	-	2, 11	110×10^3	115×10^3	1.13	1.10	-[a]
28	0.5	-	-	3, 12	90×10^3	100×10^3	1.14	1.10	-[a]
29	0.5	162	99.5	1, 10	180×10^3	185×10^3	2.88	2.70	5.6
30	0.5	162	99.5	2, 11	105×10^3	112×10^3	2.92	2.68	5.8
31	0.5	162	99.5	3, 12	80×10^3	88×10^3	2.87	2.66	5.9
Raw cotton fabric					1.1×10^9	-[a]	-[a]	-[a]	-[a]

[a]: Test was not performed.

and heated for 45 min at 70 ºC. Then, the fabric was dried at 80 ºC for 30 min.

Synthesis of Magnetite Nanoparticles and Reduction of Graphene Oxide on Cotton Fabric

Pre-calculated amounts of $FeCl_3$ and $FeCl_2$ (Fe^{2+}/Fe^{3+} molar ratio=2) were dissolved in 100 m*l* distilled water at ambient temperature under vigorous stirring using magnetic stirrer. The graphene oxide coated samples or raw cotton fabrics were immersed into the solutions. Next, different amounts of sodium hydroxide were slowly added to the aqueous solution under constant stirring, and the temperature was then increased. The solution was stirred at 90 ºC for 120 min. The treated fabrics were dried at 60 ºC for 30 min followed by curing at 140 ºC for 3 min. Finally, the treated fabrics were washed with distilled water and dried at ambient temperature.

The exact formation and tests results for each sample examined in this study are summarized in Table 1.

Instruments and Test Methods

Microscopic images and EDS patterns were established by field emission scanning electron microscope (MIRA3-TESCAN, Czech Republic) and scanning electron microscope (LEO 440i, UK). X-ray diffraction analysis (XRD) was performed with a Bruker D8 Discover X-ray diffractometer using a Cu Kα radiation source (λ=1.5410 Å) operating at 40 kV and 30 mA. X-ray photoelectron spectroscopy (XPS) measurements were done on an X-ray 8025-BesTec XPS system (Germany) with an Al Ka X-ray source ($h\upsilon$= 1,486.6 eV). Electrical surface resistivity of the fabrics was determined based on AATCC test method 76-2005 by means of the Sairan Digital Multimeter, model 8515, Iran. Magnetization was evaluated by utilizing a vibrating sample magnetometer at room temperature. UV-blocking activities of the fabrics were evaluated according to AATCC Test Method 183-2004 (transmittance or blocking of erythemally weighted ultraviolet radiation through fabrics) by using Perkin-Elmer Lambda 35 UV-vis spectrophotometer.

The burning method was used to determine the percentage of the nanocomposite on weight of fabric (o.w.f.). Weight-treated samples were placed in a porcelain crucible and kept in an oven with a range of room temperature to 600 ºC for 140 min. The calculations were conducted in such a manner that the remainder weight was subtracted from the remainder weight of the blank sample, and then the percentage was obtained.

To evaluate the durability of coatings on cotton, the electrical surface resistivity and the percentage of the nanomaterials on samples were measured after laundering. The treated samples with 0.5 % of the graphene oxide were washed according to the AATCC Test Method 61-2003 Test No. 2A using AATCC Standard Instrument Atlas Launder-Ometer LEF. An AATCC Standard Reference Detergent WOB was used. The treated samples were subject to 5 cycles of consecutive washing. At the end of the 5th cycle, the samples were rinsed with distilled water and air-dried. In this approach, each cycle of washing process is equivalent to five home machine launderings according to the AATCC Test Method.

The physical properties of the cotton fabrics such as tensile strength, elongation, crease recovery angle and stiffness were evaluated using the standard testing procedures. Tensile properties of the samples were measured according to ASTM D 5035 strip test method. Crease recovery angle (warp+filling) of the fabric samples was determined according to a method prescribed by American Association of Textile Chemist and Colorists (AATCC test method 66-2008) with specimen size 40 mm×15 mm. Fabric stiffness as expressed in terms of bending length was measured according to ASTM D 1388-96 (2002) test method. The bending rigidity of the fabrics was calculated using equation (1).

$$G = M \times (C)^3 \quad (1)$$

where G is the bending rigidity (mg·cm), M fabric weight (mg/cm^2) and C, average bending length (cm).

The antibacterial properties of the cotton samples were measured by AATCC 100-2004 test method against *Escherichia coli* (*E. coli*, ATCC 25922, Gram-negative bacterium) and *Staphylococcus aureus* (*S. aureus*, ATCC 25923, Gram-positive bacterium) as common pathogenic bacterium. Antibacterial activity was expressed in terms of the percentage reduction of the microorganisms and calculated as:

$$\text{Percentage reduction of microorganisms (R)\%} = (A - B)/A \times 100 \quad (2)$$

where, A and B are the number of microorganisms colonies on untreated and treated fabrics, respectively.

Results and Discussion

Characterization

Microscopic images of various cotton fabrics including untreated, treated with graphene oxide, and treated with reduced graphene oxide/magnetite nanocomposite are presented in Figures 1 and 2. It is thoroughly possible to recognize the graphene oxide nanosheets on the surface of graphene oxide treated sample *via* comparing Figure 1(A) with Figure 1(B). The treated cotton fabric with a graphene oxide surface displayed some corrugations (Figure 1(B)), while the surface of the untreated cotton fabric was clean and smooth (Figure 1(A)). The surfaces of the treated cotton with reduced graphene oxide/magnetite nanocomposite were completely coated by the nanocomposite condensed as layer (Figure 1(C)). FE-SEM was employed to confirm the nanocomposite loading on the surface of the cotton fabric. The presence of magnetite nanoparticles on the surface of the cotton fabric is illustrated in Figures 2(C). It reveals that

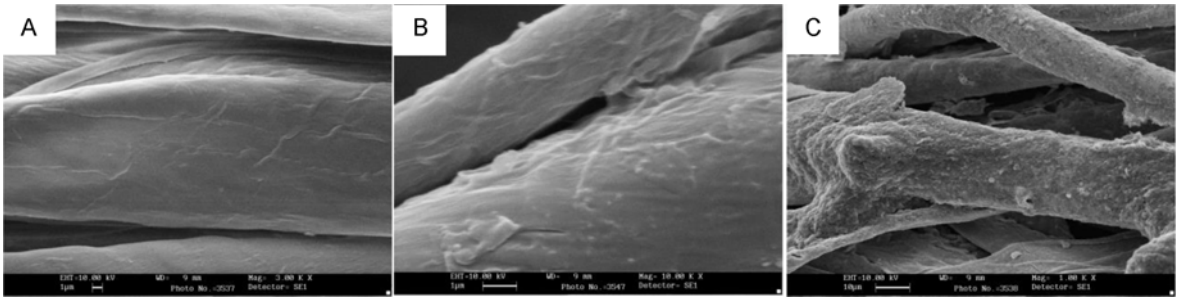

Figure 1. SEM images of various cotton fabrics; (A) raw, (B) treated with graphene oxide (sample 18), and (C) treated with reduced graphene oxide/magnetite nanocomposite (sample 24).

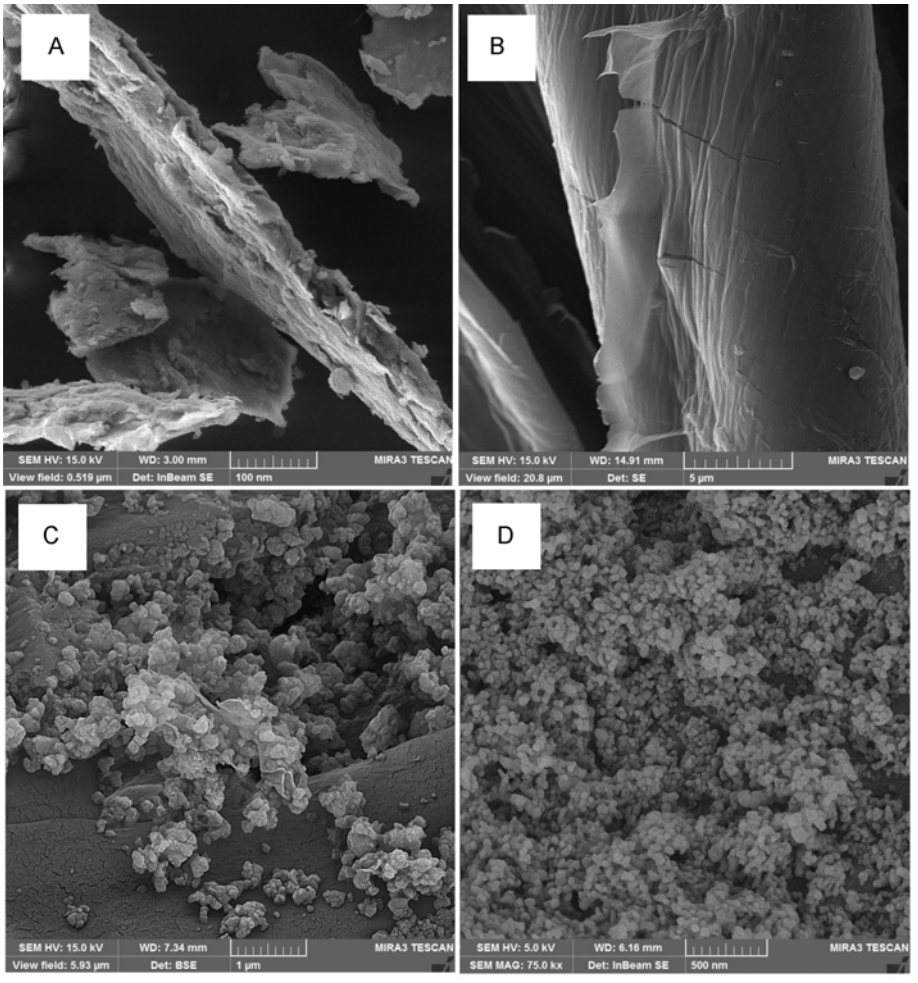

Figure 2. FE-SEM images of (A) graphene oxide and treated cotton fabrics with (B) graphene oxide (sample 18) and (C and D) reduced graphene oxide/magnetite nanocomposite (sample 24).

reduced grap hene oxide nanosheets are decorated with magnetite nanoparticles. The image at higher magnification indicates the presence of spherical-shaped magnetite particles, with average sizes in the range of 8-12 nm (Figure 2(D)). Figure 2(A) shows FE-SEM image of the obtained graphene oxide, which illustrating their flake-like shape. The graphene oxide can be also observed on the cotton fabric (Figure 2(B)).

The successful formation of the magnetite nanoparticles on the treated fabrics was verified by the chemical compositions analyzed by EDS. As shown in Figure 3, iron is an element on the treated sample apart from the carbon

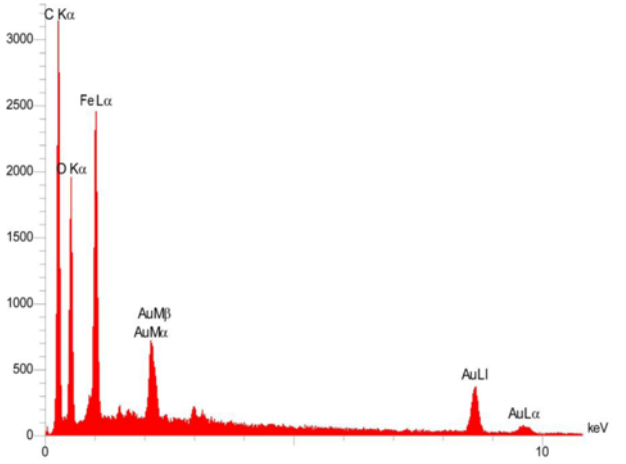

Figure 3. EDS spectrum of treated cotton fabric with reduced graphene oxide/magnetite nanocomposite (sample 24).

and oxygen that relates to the reduced graphene oxide and cotton. As the fabrics were coated by gold layer before SEM observation, Au peaks are also included in the spectra. Also, the X-ray mappings of the treated cotton with reduced graphene oxide/magnetite nanocomposite employed to

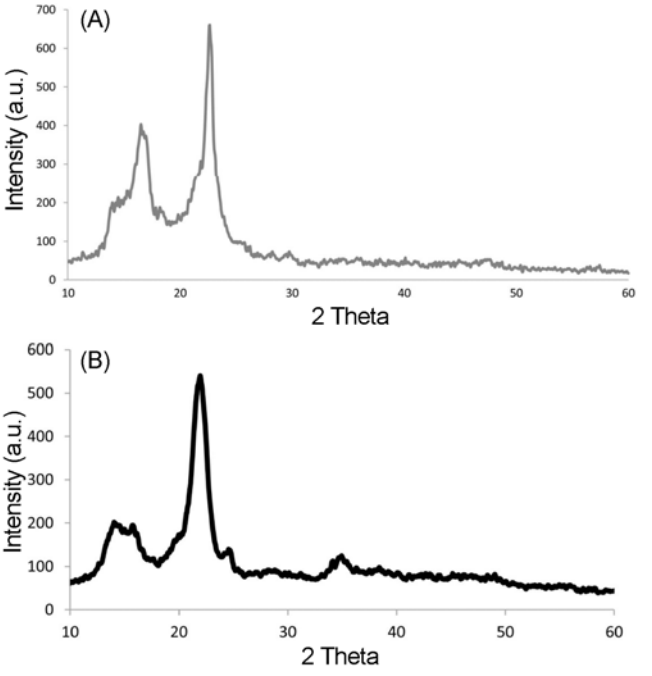

Figure 5. XRD patterns of (A) raw and (B) treated cotton fabric with reduced graphene oxide/Fe_3O_4 nanocomposite (sample 24).

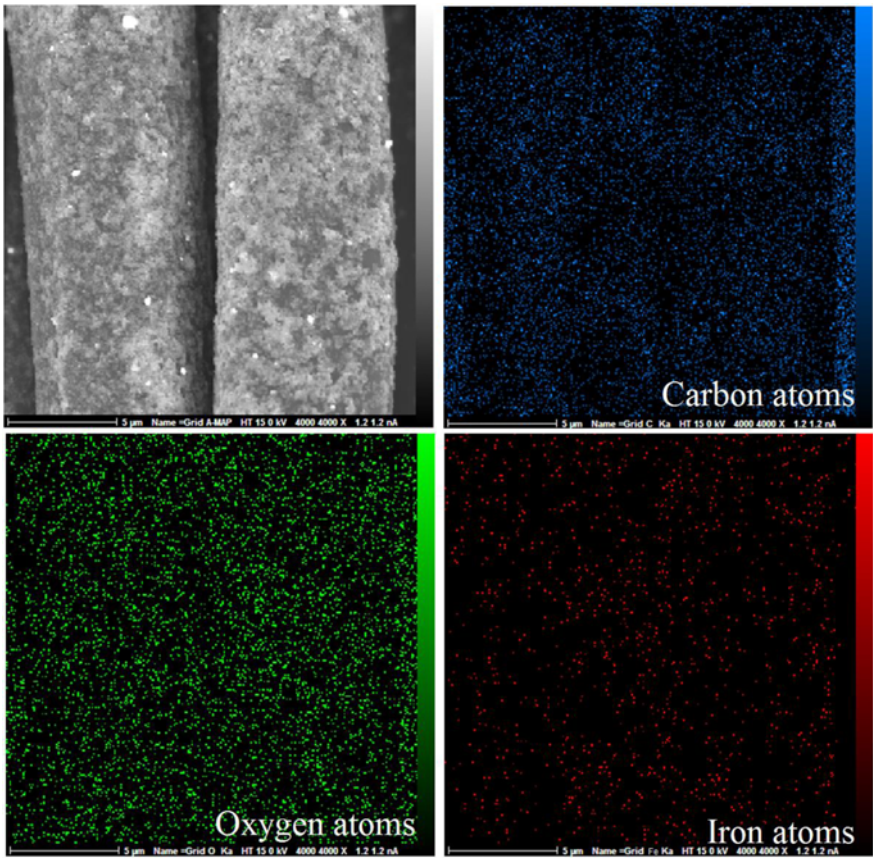

Figure 4. Microscopic and X-ray mapping images of treated cotton fabric with reduced graphene oxide/Fe_3O_4 nanocomposite (sample 24).

investigate the distribution of elements on the fabric surface and results presented in Figure 4. It is clearly observed that the distribution of iron atoms on the sample is uniform.

XRD patterns were used to study crystalline status of the nanocomposite on the fabric surface (Figure 5). The peaks at 2θ values of 13°, 16° and 22.8° are the diffraction peaks of the cellulose, which is a main substrate. The treated fabric confirmed the formation of cubic spinel structure of Fe_3O_4 in the XRD pattern. The successful synthesis of magnetite particles on the cotton fabrics can be established by the characteristic peak at 2θ value of 35.3°. Also, no obvious diffraction peaks of graphene oxide can be seen, possibly because the main peak at 2θ=12.8° was covered by the main peak of cotton. Moreover, the patterns in Figure 5 make it clear that the peak intensities of treated cotton in comparison with similar cases of raw cotton are weaker. This might be attributed to nanocomposite coatings on cotton which act as a shield against X-ray radiation.

Stability of the coatings is a particular requirement for textiles because they are subject to frequent washing, and hence the use of a suitable coating condition is necessary. Table 1 exhibit the burning test results of coated cotton fabric (with 0.5 % graphene oxide) before and after washing. Based on the obtained results, the reduction in ash percentage of the coated cotton fabrics after 25 cycles of washing was negligible and the nanocomposite have proper adherence to cotton samples.

The coloring effect of the applied treatment on the fabrics was evaluated by reflectance spectrophotometer according to the CIELAB system. L^* (lightness), a^* (redness-greenness) and b^* (yellowness-blueness) color values of raw and treated cotton were presented in Table 2. The raw cotton had white color with a high L^* value and negligible a^* and b^* values. During the treatment, the color of the cotton sample changed to brown or gray due to the synthesis of graphene oxide and reduced graphene oxide/Fe_3O_4 nanocomposite, respectively. After treatment with graphene oxide, b^* values were 12.09, which confirmed the brown color of the fabrics. The treated fabrics with graphene oxide had the highest b^* value confirming the brown color. The nanocomposite-treated fabric had the lowest reflectance with negligible a^* and b^* values confirming the gray color.

When the cotton fabric was immersed in a graphene oxide suspension, it was quickly coated with the graphene oxide sheets. The white color of the cotton changed to brown, confirming the uniform coating of cotton fabric by graphene oxide. As the basal planes and edges of graphene oxide are rich in carboxyl and hydroxyl functional groups it is reasonable to postulate that it can adhere strongly to the cellulose fibers through forming hydrogen bonds with the hydroxyl groups. In previous works, the hydrogen bonding interaction between the oxygen groups on graphene oxide and the hydroxyl groups in the cellulose has been confirmed [32-34].

Table 2. Color coordinates of various cotton fabrics

Sample	L^*	a^*	b^*
Raw cotton	83.90	-0.11	-0.26
Graphene oxide coated cotton (sample 18)	75.65	2.22	12.09
reduced graphene oxide/Fe_3O_4 nanocomposite coated cotton (sample 24)	46.02	0.45	2.48

The reduced graphene oxide/magnetite nanocomposite was prepared on cotton surface by chemical deposition of iron ions using graphene oxide as carriers. The method is that Fe^{3+}/Fe^{2+} ions in the proper ratio were captured by anions groups on the graphene oxide sheets by coordination and then magnetite nanoparticles on graphene oxide were precipitated by treating iron ions coordinated with graphene oxide with sodium hydroxide [35]. The relevant chemical reaction can be expressed as follows:

$$Fe^{2+} + 2Fe^{3+} + 8OH^- \rightarrow Fe_3O_4 + 4H_2O \quad (3)$$

Considering the alkalinity of the process, the reduction of the graphene oxide occurred along with the magnetite nanoparticles synthesis in the presence of sodium hydroxide. Consequently, the color of the treated cotton fabric changed from brown to gray (Scheme 1).

Similar to the reduction of graphene oxide in acidic solutions, alkaline solutions are also very efficient for the deoxygenation of graphene oxide. Fan *et al.* showed that reduced graphene oxide suspension could be prepared by

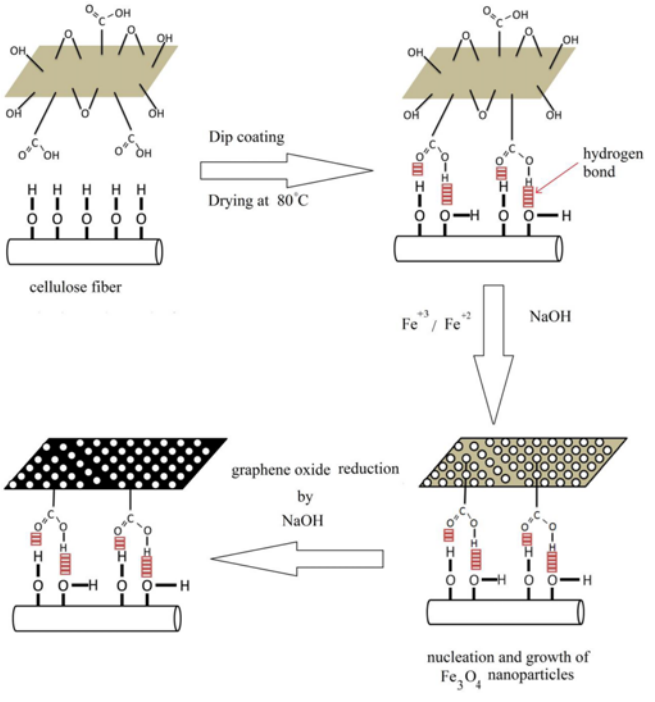

Scheme 1. The proposed mechanism of reduced graphene oxide/Fe_3O_4 nanocomposite synthesized on cotton fiber.

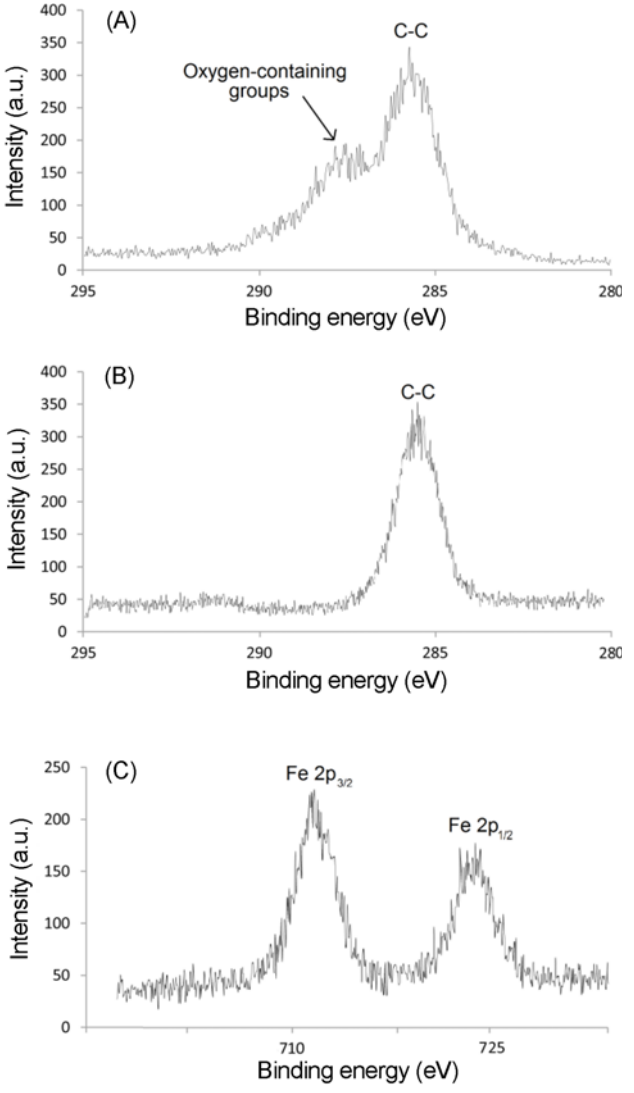

Figure 6. XPS spectra of graphene oxide and reduced graphene oxide/Fe_3O_4 nanocomposite; (A) C 1s spectrum of graphene oxide, (B) C 1s spectrum of the nanocomposite, and (C) Fe 2p spectrum of the nanocomposite.

simply heating a graphene oxide suspension under strongly alkaline conditions (in presence of NaOH or KOH) at moderate temperatures (50-90 ºC). Although the proposed mechanism is unclear, it has been shown that dispersed graphene oxide undergoes faster reduction as the concentration of sodium hydroxide or potassium hydroxide increases [36].

The reduction of the graphene oxide and formation of magnetite nanoparticles on cotton surface was studied by X-ray photoelectron spectroscopy (XPS). Figure 6 clearly shows that the O/C ratio in the reduced graphene oxide/ magnetite nanocomposite (Figure 6(B)) decreases remarkably compared with that of graphene oxide (Figure 6(A)), and that most of the oxygen groups were successfully removed. In the Fe 2p spectrum (Figure 6(C)), the peaks for Fe $2p_{3/2}$ and Fe $2p_{1/2}$ were observed at 711.2 and 724.8 eV, which is also indicative of the formation of magnetite. Consequently, the results established the considerable reduction of graphene oxide and the successful preparation of the reduced graphene oxide/Fe_3O_4 nanocomposite.

Fabrics Properties

Electrical properties and magnetic properties of the treated cotton with reduced graphene oxide/Fe_3O_4 nanocomposite were investigated to compare with the treated cotton with either reduced graphene oxide or magnetite nanoparticles.

The electrical resistivity variation of cotton samples are presented in Table 1. The raw cotton and graphene oxide treated cotton fabrics were not electroconductive (electrical resistivity in the range of 1×10^9-2×10^9 ohm/square). After reduction of graphene oxide coated cotton fabrics by sodium hydroxide (NaOH), the electrical resistivity of the samples was reduced, in other words, its electrical conductivity increased, which indicated the reduction of oxygen functional groups from the graphene oxide. The electrical resistivity of treated cotton samples decreased from 360×10^6 ohm/square to 90×10^3 ohm/square by increasing the amount of graphene oxide from 0.1 w/v % to 0.5 w/v % in the impregnating bath. The electrical conductivity of these samples arises mainly from the reduced graphene sheets. The increase in graphene oxide concentration had a tangible effect on electrical conductivity of the coated fabrics due to the higher reduced graphene content that produces a better contact between the reduced graphene sheets. Furthermore, based on the obtained results, the electrical conductivity of the treated fabrics with reduced graphene oxide/magnetite nanocomposite becomes slightly higher than treated samples with reduced graphene oxide, which might be due to the conductivity of the magnetite nanoparticles [37]. The geometry of reduced graphene oxide is planar and of magnetite is spherical. Many spaces existed among the reduced graphene oxide from the inherent surface roughness of the cotton fibers, so no efficient interconnection existed between them. Coating with magnetite partially filled these spaces. Moreover, as shown in Table 1, laundering did not cause any remarkable changes in electrical resistivity of the treated samples with 0.5 % graphene oxide.

The values of the saturation magnetization of treated fabrics with magnetite nanoparticles were measured using vibrating sample magnetometry at room temperature. Samples were placed at the applied magnetic field (H), 0-8000 Oe. The magnetization rapidly increases with the increase in magnetic field, then turns flat at different values of applied magnetic field, and saturation magnetization values of each treated samples were measured using vibrating sample magnetometry. The values of the saturation magnetization of treated cotton fabrics are given in Table 1. The values of the saturation magnetization obtained in the literature by other authors have been: Zhang and coworkers

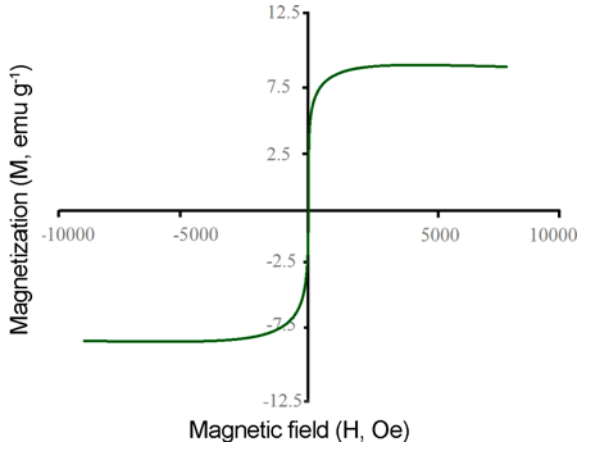

Figure 7. Room-temperature magnetization curve of treated cotton fabric (sample 10).

reported the hydrothermal synthesis of magnetite nanoparticles on polyester fabric and created a magnetic fabric with the saturation magnetization of 38 emu g^{-1} [14]. Harifi and Montazer treated polyester fabrics with Fe_3O_4 nanoparticles and produced a magnetic fabric with saturation magnetization of 7.5 emu g^{-1} [15]. Nazari *et al.* reported saturation magnetization values ranging from 4.6 to 7.8 emu g^{-1} for wool fabrics coated with Fe_3O_4 nanoparticles [16]. The value of the saturation magnetization obtained in this study ranged from 5.6 to 7.8 emu g^{-1}, which is in line with the previous observations. The hysteresis loop of the treated cotton fabric with Fe_3O_4 nanoparticles (sample 10) at room temperature are shown in Figure 7. It is apparent that the magnetic hysteresis loop was narrow for the treated fabrics and extremely small coercivity (H_c=15 Oe) and remanence values (M_r=1.00 emu g^{-1}) were obtained for the iron oxide nanoparticles synthesized on the fabrics indicating the almost superparamagnetic nature of these particles.

Based on the obtained results, the saturation magnetization of the nanocomposite coated cotton decreases as the reduced graphene oxide content increases. The saturation magnetization of treated samples decreased from 7.8 emu g^{-1} to 5.6 emu g^{-1} by increasing the amounts of graphene oxide in the impregnating bath. This could be attributed to the presence of magnetically inactive reduced graphene oxide sheets at the nanocomposite. It can be concluded that the magnetic properties of the treated fabrics could be finely tuned by controlling the concentration of graphene oxide.

However, the magnetic properties of the nanocomposite treated fabric are similar to that of the Fe_3O_4 nanoparticles loaded on cotton fabric. Both of the samples exhibit a superparamagnetic behavior, which is due to the presence of magnetite with small particle size (less than 25 nm) [38].

In order to investigate the physical properties of treated fabrics, crease recovery angle, bending length, bending rigidity, tensile strength and elongation were estimated. The results are presented in Table 3. The results acquired indicate that the application of reduced graphene oxide/Fe_3O_4 nanocomposite (sample 24) did not have a considerable effect on wrinkle resistance of the treated cotton fabric as compared to the untreated fabric. The bending lengths of raw cotton and coated cotton samples are very close. However, the samples coated with the nanocomposite had the lowest bending length and bending rigidity. This can be attributed to the presence of nanocomposite between the fibers that restricted the swelling of the fibers, thereby reducing the stiffness of the fabrics [39].

Cotton has an excellent resistance to alkalis. However, after reduction of graphene oxide coated cotton samples by sodium hydroxide, the tensile strength of the sample was decreased, which could be attributed to the treatment condition (90 ºC, 120 min). The difference in tensile strength between the untreated and the nanocomposite-treated cotton fabric (sample 24) was a reduction of 7.5 %.

Magnetite nanoparticles possess unique characteristics such as photocatalytic, magnetic, antifungal and antibacterial, which can make it possible to produce a textile with multifunctional properties. Moreover, Fe_3O_4 naoparticles is bio-safe and biocompatible for applications in medicine textile [40]. The Fe_3O_4 treated textile can inhibit the growth of bacteria possibly by two mechanisms. The first important reason is the production and penetration of reactive oxygen species, which causing bacterial cell oxidation and subsequent bacterial death. The second reason is the strong electrostatic attraction toward bacterial outer membranes resulting in binding of magnetite nanoparticles to bacterial cell walls causing membrane disruption [41].

The antibacterial activities of the samples were evaluated quantitatively by suspension method against both *E. coli* and *S. aureus* bacteria. The percentage of the bacteria reduction by Fe_3O_4 treated, reduced graphene oxide/Fe_3O_4 nanocomposite treated and raw cotton samples are reported in Figure 8. The raw cotton fabrics provide a suitable media for growth of microorganisms. The antibacterial efficiencies of the Fe_3O_4

Table 3. Physical properties of treated and untreated cotton fabrics

Sample	Crease recovery angle (°)	Bending length (cm)	Bending rigidity (mg·cm)	Tensile strength (N)	Elongation (mm)
Raw cotton	144	1.30	23.72	292.09	20.3
Cotton-reduced graphene oxide/Fe_3O_4 (sample 24)	142	1.10	14.56	270.11	33.3

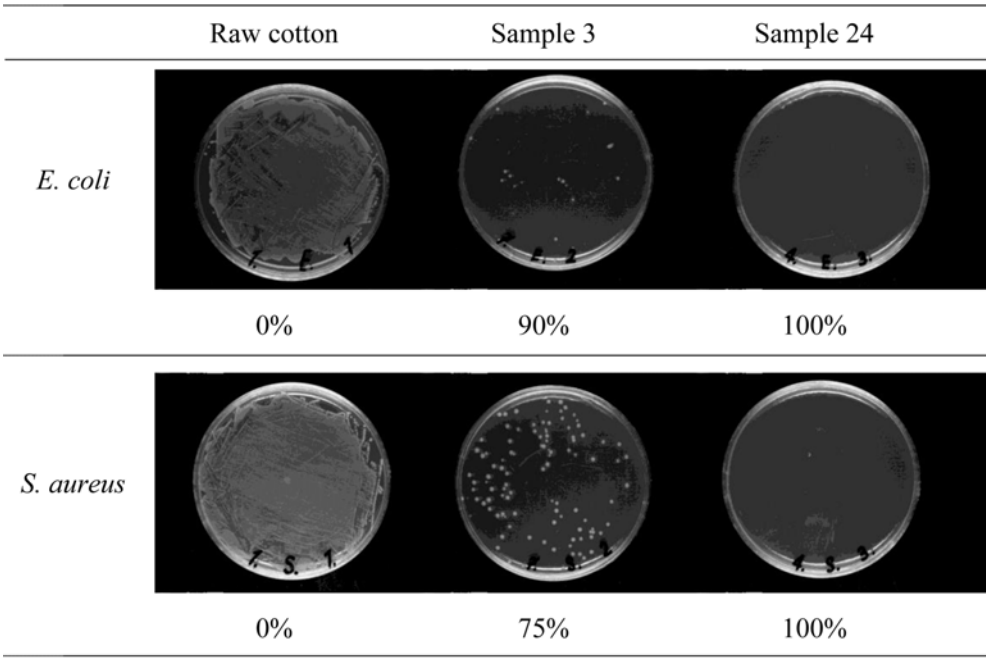

Figure 8. The antibacterial efficiency of raw and treated cotton samples.

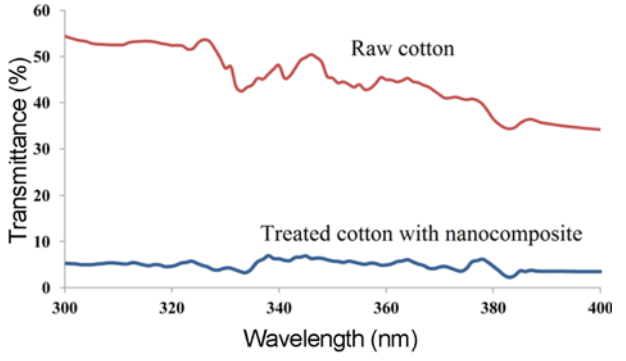

Figure 9. UV transmittance spectra of raw cotton fabric and treated cotton fabric with reduced graphene oxide/Fe_3O_4 nanocomposite (sample 24).

and the nanocomposite treated fabrics against *E. coli* bacteria were 90 % and 100 %, respectively. Also, antibacterial activity of the nanocomposite treated sample against *S. aureus* was higher than Fe_3O_4 treated samples, which is due to the high surface area of reduced graphene oxide. Adding reduced graphene nanosheets to magnetic nanoparticles can facilitate effective bacterial decomposition by increasing the contact between the Fe_3O_4 nanoparticles and the bacteria [26].

In addition, we were surprised to find that high antibacterial efficiency, good electrical conductivity and superparamagnetic properties were not the superior aspects of the nanocomposite treated cotton; these samples likewise had proper UV blocking activity. The UV transmittance spectra of blank cotton and treated cotton fabric with reduced graphene oxide/Fe_3O_4 nanocomposite were illustrated in Figure 9. The nanocomposite treated cotton fabric had much lower UV transmittance compared to the raw cotton fabric. This could be attributed to the UV absorption ability of reduced graphene oxide nanosheets [24]. Also, the UV protection factor (UPF) values were calculated using mean percentage transmission in the UV-A (320-400 nm) and UV-B (280-320 nm) regions. The UPF value of the blank cotton sample was 11.12. An UPF value of <15 indicated no protection against transmittance of UV radiation through fabric onto skin. For the nanocomposite treated cotton fabric, the UV transmittance decreased significantly and UPF value increased to 266.02, showing its excellent ability to block UV radiation.

Conclusion

In this study, for the first time the reduced graphene oxide/magnetite nanocomposite was used for fabrication of multifunctional cotton fabrics. Cotton fabrics with magnetic property, electrical conductivity, proper antimicrobial properties and UV blocking activity were obtained. Through SEM and X-ray mapping images, XPS spectra, XRD and EDS patterns the successful formation of the reduced graphene oxide/magnetite nanocomposite on cotton surface was verified. The combination of magnetite nanoparticles with reduced graphene oxide nanosheets in finishing process led to exploit the properties of either Fe_3O_4 nanoparticles or reduced graphene oxide on cotton fabrics. It is expected reduced graphene oxide/magnetite nanocomposite coated fabrics can be used as smart textiles, especially in those fields associated with weave, electronics, biology, medicine, food, life, clothes, aviation, and military.

References

1. Q. A. Pankhurst, N. T. K. Thanh, S. K. Jones, and J. Dobson, *J. Phys. D: Appl. Phys.*, **42**, 224001 (2009).
2. A. S. Teja and P. Y. Koh, *Progr. Cryst. Growth Ch.*, **55**, 22 (2009).
3. H. El Ghandoor, H. M. Zidan, M. M. Khalil, and M. I. M. Ismail, *Int. J. Electrochem. Sci.*, **7**, 5734 (2012).
4. Q. A. Pankhurst, J. Connolly, S. K. Jones, and J. J. Dobson, *J. Phys. D: Appl. Phys.*, **36**, R167 (2003).
5. S. Peng and S. Sun, *Angew. Chem.*, **119**, 4233 (2007).
6. O. Veiseh, J. W. Gunn, and M. Zhang, *Adv. Drug Deliv. Rev.*, **62**, 284 (2010).
7. X. Wang, R. Zhang, C. Wu, Y. Dai, M. Song, S. Gutmann, F. Gao, G. Lv, J. Li, X. Li, and Z. Guan, *J. Biomed. Mater. Res. A*, **80**, 852 (2007).
8. K. Jia, R. Zhao, J. Zhong, and X. Liu, *J. Magn. Magn. Mater.*, **322**, 2167 (2010).
9. R. Dhawan, S. Kumari, R. Kumar, S. K. Dhawan, and S. R. Dhakate, *RSC Adv.*, **5**, 43279 (2015).
10. J. Liang, Y. Huang, J. Oh, M. Kozlov, D. Sui, S. Fang, R. H. Baughman, Y. Ma, and Y. Chen, *Adv. Funct. Mater.*, **21**, 3778 (2011).
11. N. Lee and T. Hyeon, *Chem. Soc. Rev.*, **41**, 2575 (2012).
12. H. Zhang and G. Zhu, *Appl. Surf. Sci.*, **258**, 4952 (2012).
13. Y. Li, J. Lan, R. Guo, M. Huang, K. Shi, and D. Shang, *Fiber. Polym.*, **14**, 1657 (2013).
14. H. Zhang, Y. Liu, and Y. Zhou, *J. Text. Inst.*, **106**, 1078 (2015).
15. T. Harifi and M. Montazer, *J. Mater. Chem. B*, **2**, 272 (2014).
16. A. Nazari, M. R. Shishehbor, and S. M. Poorhashemi, *J. Text. Inst.*, DOI:10.1080/00405000.2015.1131439, 2016.
17. M. J. Allen, V. C. Tung, and R. B. Kaner, *Chem. Rev.*, **110**, 132 (2009).
18. W. W. Liu, X. B. Yan, J. W. Lang, C. Peng, and Q. J. Xue, *J. Mater. Chem.*, **22**, 17245 (2012).
19. Z. Lu, C. Mao, and H. Zhang, *J. Mater. Chem. C*, **3**, 4265 (2015).
20. I. A. Sahito, K. C. Sun, A. A. Arbab, M. B. Qadir, and S. H. Jeong, *Electrochim. Acta*, **173**, 164 (2015).
21. I. A. Sahito, K. C. Sun, A. A. Arbab, M. B. Qadir, and S. H. Jeong, *Carbohydr. Polym.*, **130**, 299 (2015).
22. K. Javed, C. M. A. Galib, F. Yang, C. M. Chen, and C. Wang, *Synth. Met.*, **193**, 41 (2014).
23. J. Molina, J. Fernández, M. Fernandes, A. P. Souto, M. F. Esteves, J. Bonastre, and F. Cases, *Synth. Met.*, **202**, 110 (2015).
24. L. Qu, M. Tian, X. Hu, Y. Wang, S. Zhu, X. Guo, G. Han, X. Zhang, K. Sun, and X. Tang, *Carbon*, **80**, 565 (2014).
25. M. Tian, X. Hu, L. Qu, S. Zhu, Y. Sun, and G. Han, *Carbon*, **96**, 1166 (2016).
26. L. Karimi, M. E. Yazdanshenas, R. Khajavi, A. Rashidi, and M. Mirjalili, *Cellulose*, **21**, 3813 (2014).
27. L. Karimi, M. E. Yazdanshenas, R. Khajavi, A. Rashidi, and M. Mirjalili, *Appl. Surf. Sci.*, **332**, 665 (2015).
28. J. Molina, F. Fernandes, J. Fernández, M. Pastor, A. Correia, A. P. Souto, J. O. Carneiro, V. Teixeira, and F. Cases, *Mater. Sci. Eng. B*, **199**, 62 (2015).
29. M. A. Shirgholami, L. Karimi, and M. Mirjalili, *Fiber. Polym.*, **17**, 220 (2016).
30. L. Karimi, M. E. Yazdanshenas, R. Khajavi, A. Rashidi, and M. Mirjalili, *J. Text. Inst.*, **107**, 1122 (2016).
31. V. Babaahmadi and M. Montazer, *Colloid Surf. A-Physicochem. Eng. Asp.*, **506**, 507 (2016).
32. Y. Feng, X. Zhang, Y. Shen, K. Yoshino, and W. Feng, *Carbohydr. Polym.*, **87**, 644 (2012).
33. M. Shateri-Khalilabad and M. E. Yazdanshenas, *Cellulose*, **20**, 963 (2013).
34. K. Krishnamoorthy, U. Navaneethaiyer, R. Mohan, J. Lee, and S.-J. Kim, *Appl. Nanosci.*, **2**, 119 (2012).
35. X. Yang, X. Zhang, Y. Ma, Y. Huang, Y. Wang, and Y. Chen, *J. Mater. Chem.*, **19**, 2710 (2009).
36. X. Fan, W. Peng, Y. Li, X. Li, S. Wang, G. Zhang, and F. Zhang, *Adv. Mater.*, **20**, 4490 (2008).
37. J. Liang, Y. Xu, D. Sui, L. Zhang, Y. Huang, Y. Ma, F. Li, and Y. Chen, *J. Phys. Chem. C*, **114**, 17465 (2010).
38. J. W. Lee, R. Viswan, Y. J. Choi, Y. Lee, S. Y. Kim, J. Cho, Y. Jo, and J. K. Kang, *Adv. Funct. Mater.*, **19**, 2213 (2009).
39. C. W. M. Yuen, S. K. A. Ku, Y. Li, Y. F. Cheng, C. W. Kan, and P. S. R. Choi, *J. Text. Inst.*, **100**, 173 (2009).
40. B. I. Kharisov, H. R. Dias, O. V. Kharissova, V. M. Jiménez-Pérez, B. O. Perez, and B. M. Flores, *RSC Adv.*, **2**, 9325 (2012).
41. M. Rastgoo, M. Montazer, R. M. Malek, T. Harifi, and M. M. Rad, *Ultrason. Sonochem.*, **31**, 257 (2016).